



■ INFECTION

The combination of silver-containing hydroxyapatite coating and vancomycin has a synergistic antibacterial effect on methicillin-resistant *Staphylococcus aureus* biofilm formation

**A. Hashimoto,
H. Miyamoto,
T. Kobatake,
T. Nakashima,
T. Shobuike,
M. Ueno,
T. Murakami,
I. Noda,
M. Sonohata,
M. Mawatari**

Department of
Orthopaedic Surgery,
Faculty of Medicine,
Saga University,
Saga, Japan

Aims

Biofilm formation is intrinsic to prosthetic joint infection (PJI). In the current study, we evaluated the effects of silver-containing hydroxyapatite (Ag-HA) coating and vancomycin (VCM) on methicillin-resistant *Staphylococcus aureus* (MRSA) biofilm formation.

Methods

Pure titanium discs (Ti discs), Ti discs coated with HA (HA discs), and 3% Ag-HA discs developed using a thermal spraying were inoculated with MRSA suspensions containing a mean in vitro 4.3 (SD 0.8) $\times 10^6$ or 43.0 (SD 8.4) $\times 10^5$ colony-forming units (CFUs). Immediately after MRSA inoculation, sterile phosphate-buffered saline or VCM (20 $\mu\text{g}/\text{ml}$) was added, and the discs were incubated for 24 hours at 37°C . Viable cell counting, 3D confocal laser scanning microscopy with Airyscan, and scanning electron microscopy were then performed. HA discs and Ag HA discs were implanted subcutaneously in vivo in the dorsum of rats, and MRSA suspensions containing a mean in vivo 7.2 (SD 0.4) $\times 10^6$ or 72.0 (SD 4.2) $\times 10^5$ CFUs were inoculated on the discs. VCM was injected subcutaneously daily every 12 hours followed by viable cell counting.

Results

Biofilms that formed on HA discs were thicker and larger than those on Ti discs, whereas those on Ag-HA discs were thinner and smaller than those on Ti discs. Viable bacterial counts in vivo revealed that Ag-HA combined with VCM was the most effective treatment.

Conclusion

Ag-HA with VCM has a potential synergistic effect in reducing MRSA biofilm formation and can thus be useful for preventing and treating PJI.

Cite this article: *Bone Joint Res.* 2020;9(5):211–218.

Keywords: Biofilm, Hydroxyapatite, MRSA, Silver, Airyscan

Article focus

- We aimed to investigate the effects of silver-containing hydroxyapatite (Ag-HA) coating and vancomycin (VCM) on methicillin-resistant *Staphylococcus aureus* (MRSA) biofilm formation.
- The findings of biofilm analysis were verified using 3D confocal laser scanning microscopy (3D CLSM) with Airyscan and scanning electron microscopy (SEM).

Key messages

- Ag-HA delayed the growth cycle of biofilms and changed their structure.

- Ag-HA and VCM synergistically reduced MRSA biofilm formation.
- 3D CLSM equipped with Airyscan was a useful method for biofilm observation.

Strengths and limitations

- This is the first study to report on qualitative biofilm analyses of Ag-HA materials, as well as the effects of Ag-HA coating and VCM on MRSA biofilm formation; these findings were verified using SEM and Airyscan-equipped 3D CLSM.
- Non-coated titanium (Ti) implants were not used as controls in vivo because these

Correspondence should be sent to
A. Hashimoto;
email: 17624015@edu.cc.saga-u.
ac.jp

doi: 10.1302/2046-3758.95.
BJR-2019-0326.R1

Bone Joint Res 2020;9:211–218.

implants showed inferior osteoconductivity in a previous study, an important feature for successful cementless total hip arthroplasty. Instead, we used HA-coated Ti implants because HA coating induces early bone ingrowth and displays good osteoconductivity.

Introduction

Total hip arthroplasty (THA) is one of the most successful orthopaedic procedures improving the quality of life, affording functional gain, promoting pain relief, and enabling motion range in patients with hip osteoarthritis. As the population ages, the number of THA cases is expected to rise with an estimated 572,000 procedures to be performed annually by 2030 in the USA.¹ Prosthetic joint infection (PJI), a complication of THA, is a burden for patients and is one of the most challenging complications for surgeons. It requires surgical resection and revision arthroplasty in severe cases, prolonging hospitalization and increasing treatment costs.² PJI reportedly occurs in 0.2% to 1.1% of primary THAs,³ prolonging the hospitalization time by up to 176% and increasing treatment costs by up to 134%.² More than 60% of PJI cases after arthroplasty are caused by either methicillin-susceptible *Staphylococcus aureus* (MSSA) or methicillin-resistant *S. aureus* (MRSA).⁴ Surgical wound infections caused by MRSA require longer hospitalization and entail higher costs than those caused by other microorganisms.²

Titanium (Ti), stainless steel, and cobalt-chrome are commonly used orthopaedic implant materials. Many orthopaedic implants are coated with hydroxyapatite (HA) to accelerate early bone ingrowth and improve osteoconductivity.⁵ However, such metal and HA surfaces are susceptible to adhesion and colonization by biofilm-forming bacteria.⁶ To kill bacteria with biofilms, antibiotic concentrations 1,000 times higher than those used for planktonic cells are required.⁷

Biofilm formation is intrinsic to PJI, but PJI is highly resistant to antibiotics. Therefore, an important anti-PJI strategy involves preventing initial bacterial adhesion to the implant surface. Consequently, various antibacterial coatings have been developed, including those incorporating vancomycin (VCM), gentamicin, chlorhexidine HA, silver (Ag), and chitosan.⁸ Ag, a well-known antibacterial coating, exhibits a broad-spectrum activity against both gram-positive and gram-negative bacteria, fungi, protozoans, and viruses.^{9,10} Further, Ag is far less likely to elicit bacterial resistance than antibiotics and shows relatively low toxicity toward humans.^{9,10} An Ag-coated megaprosthesis has been applied in the field of orthopaedic surgery.¹¹ However, Ag in high concentrations is toxic to osteoblasts, suppresses ossification, and is involved in osteolysis and postoperative prosthesis loosening.^{11–14} Therefore, insertion of the prosthesis coated with Ag using conventional techniques into the bone marrow is rather difficult. Moreover, various Ag side effects, including argyria, kidney and liver damage, leukopenia, and

neurotoxicity have been reported.^{15–17} Recently, an Ag-containing HA (Ag-HA) coating was developed using a thermal spray technique.¹⁸ Other studies demonstrated inhibition of bacterial adhesion and growth on the surface of 3% Ag-HA materials,¹⁹ and the enhancement of osteoconductivity in the rat tibia using 3% Ag-HA coatings.²⁰ The biological safety of Ag-HA coatings has also been shown in previous studies.^{21,22}

However, detailed qualitative and quantitative biofilm analyses on HA and Ag-HA materials are lacking. Therefore, we proposed the development of an anti-PJI strategy as an alternative to conventional therapy using antibacterial coatings or antibiotics only. We hypothesized that the combination of antibiotics and Ag-HA would reduce bacterial biofilm formation because the characteristics of the MRSA biofilm on HA and Ag-HA may differ. Here, we evaluated the effect of Ag-HA coating and VCM on MRSA biofilm formation using viable cell counts, 3D confocal laser scanning microscopy (3D CLSM) with Airyscan, and scanning electron microscopy (SEM).

Methods

Ag-HA coating - in vitro experiments. One side of the pure Ti discs (14 mm wide, 1 mm thick; Kobe Steel, Kobe, Japan) was coated with Ag-HA, and the Ag-HA coating technique is detailed in the Supplementary Material.

Bacteria and culture conditions - in vitro experiments. We used UOEH6 (University of Occupational and Environmental Health Hospital, Fukuoka, Japan), a biofilm-producing MRSA strain was isolated from a blood sample of a septic patient at a hospital. The MRSA culture conditions are detailed in the Supplementary Material.

Microbiological evaluation by bacterial count determination - in vitro experiments. Three types of discs were prepared: Ti, Ti with HA coating (HA), and Ti with 3.0% Ag-HA coating (Ag-HA). The inverted lid of a 60 mm dish was placed in the centre of a 90 mm dish (Figure 1). Four discs of the same type were aseptically placed on the inverted lid of the 60 mm dish, and 10 µl of the MRSA suspension was inoculated onto each disc. Then, 10 µl of sterile phosphate-buffered saline (PBS) or 10 µl of 20 µg/ml VCM (Kobayashi Kakou Corp., Fukui, Japan) was

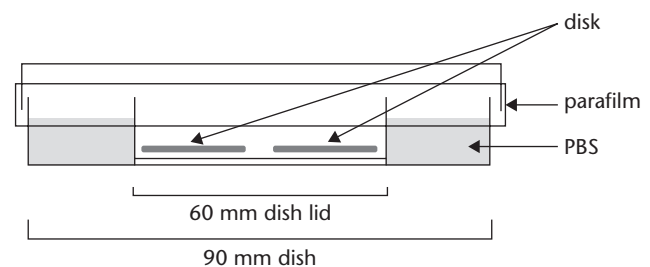


Fig. 1

Setup of the methicillin-resistant *Staphylococcus aureus* (MRSA) incubation. MRSA was incubated on the disc, ensuring that it did not dry and the discs did not contact each other. PBS, phosphate-buffered saline.

immediately added to each disc. To prevent disc drying, sterile PBS was poured between the 90 mm and 60 mm dishes, and the 90 mm dish was covered with parafilm (Figure 1). The discs were incubated for 24 hours at 37°C, agitated with a vortex mixer in 10 ml of sterile PBS, and then ultrasonically irrigated for five minutes, after which they were agitated with the vortex mixer again. Serial dilutions (ten-fold series) of the irrigated PBS solutions were plated on the agar plates and incubated for 48 hours at 37°C. The colonies were counted, and the amounts of CFUs per disc were determined. A total of 12 discs were used in each treatment group, namely Ti PBS, Ti VCM, HA PBS, HA VCM, Ag-HA PBS, and Ag-HA VCM.

3D CLSM protocol - in vitro experiments. Four discs were used in each treatment group (Ti PBS, Ti VCM, HA PBS, HA VCM, Ag-HA PBS, and Ag-HA VCM). Because biofilm dimensions varied, three sections of each disc were randomly recorded for quantitative analysis according to the method described in previous literature.^{23,24} The 3D CLSM protocol and feature of Airyscan are provided in the Supplementary Material.

SEM protocol - in vitro experiments. The SEM protocol is detailed in the Supplementary Material.

Ag-HA coating - in vivo experiments. Both sides of Ti discs (14 mm wide, 1 mm thick; Kobe Steel) were coated with Ag-HA according to the protocol used for the in vitro analysis.

Bacteria and culture conditions - in vivo experiments. The MRSA strain used was UOEH6 (University of Occupational and Environmental Health Hospital). The bacterial strain and culture conditions were the same as those used in the in vitro analysis, except that cells were resuspended in sterile PBS for in vivo experiments.

Animals. We used 12 ten-week-old male Sprague-Dawley rats from Kyudo (Kumamoto, Japan), weighing a mean 373.3 g (SD 19.9; 354 to 389). The rats were housed individually in standard cages in a temperature-controlled room (20°C to 25°C) with 12-hour light-dark cycles and acclimated for seven days before the experiments in a room in which a suitable environment was maintained. Standard rodent chow and water were provided ad libitum. Three rats were randomly assigned to each group: HA, HA VCM, Ag-HA, and Ag-HA VCM. All animal procedures were approved by the Animal Research Ethics Committee of our institution (approval number 29-044-0).

Surgical technique - in vivo experiments. The rats were anaesthetized intraperitoneally using a mixture of anaesthetic agents (0.375 mg/kg medetomidine, 2 mg/kg midazolam, and 2.5 mg/kg butorphanol).²⁵ The infection model using the dorsum of the rat was performed as previously reported.¹⁹

The back of the rat was shaved, cleaned with povidone-iodine, and dried. Four sagittal 1.5 cm incisions were made on the dorsum: two at the level of the scapula

and another two at the level of the lower rib cage. Each incision was 2 cm lateral to the midline, and the pockets made were not connected to each other.

HA and Ag-HA discs were prepared. A total of four discs of the same type were aseptically implanted one by one into the subcutaneous pocket of each rat; 20 µl of MRSA suspension was inoculated onto the discs in these pockets. The incisions were closed using interrupted 3-0 nylon suture. The rats were divided into VCM (Kobayashi Kakou Corp.) injected and VCM noninjected groups. In the VCM injected group, VCM was injected subcutaneously at a concentration of 110 mg/kg into the tail of the rats using a 23-gauge needle immediately after skin suture, ensuring that the injected drug did not flow into the implanted pocket.²⁶ After the surgery, atipamezole (0.75 mg/kg) was used to induce the recovery of animals from anaesthesia. No analgesia was used after the surgery. Next, 12 hours after the previous subcutaneous injection of VCM the second subcutaneous injection of 110 mg/kg of VCM was performed into the tail of the rat. Then, 12 hours after the second subcutaneous injection of VCM the rat was euthanized, and the dorsum of the rat was cleaned with povidone-iodine and dried. After this, the discs were aseptically removed and placed in 10 ml of sterile PBS.

Microbiological evaluation by bacterial count determination - in vivo experiments. The methods of bacterial count determination were the same as those used in the in vitro analysis and are detailed in the Supplementary Material. A total of 12 discs were used for each treatment group (HA, HA VCM, Ag-HA, and Ag-HA VCM).

Statistical analysis. All numerical data are expressed as the mean (SD). Live cell counts in vitro were analyzed with Steel's multiple comparisons test to compare the Ti PBS group with the other five groups. Those in vivo were analyzed with the same test to compare the HA PBS group with the other three groups. The total biofilm volume per area was analyzed with Dunnett's multiple comparisons test to compare the Ti PBS group with the other five groups. All analyses were performed using JMP Pro software (version 13.2.1; SAS Institute, Cary, North Carolina, USA). Statistical significance was indicated by $p < 0.05$. The sample size was determined with a priori power analysis (power = 0.80, $\alpha = 0.05$, and effect size = 0.5), showing that 48 samples were required. In the microbiological evaluation in vivo, 12 discs from three rats were used in each treatment group; the total number of discs used in the four groups was 48.

Results

Biofilm analysis using CLSM with Airyscan - in vitro experiments. As observed under CLSM with Airyscan, the biofilms of the HA PBS group were composed of clumped bacterial cells with stained cell surfaces (Figure 2). Conversely, those in the Ag-HA PBS group appeared to contain scattered

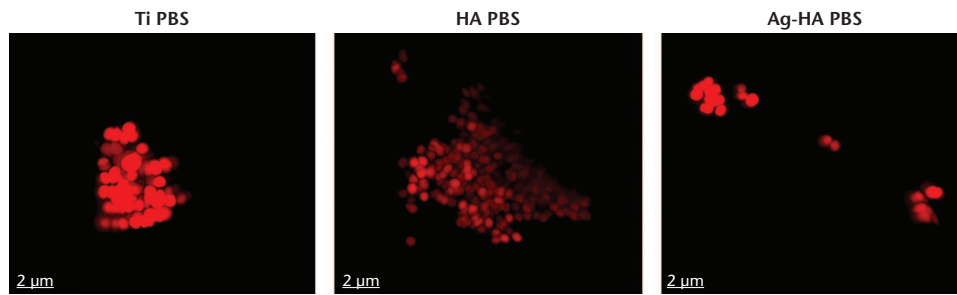


Fig. 2

Confocal laser scanning microscopy (CLSM) Airyscan images of calcein red-orange-stained methicillin-resistant *Staphylococcus aureus* (MRSA) on discs of the titanium phosphate-buffered saline (Ti PBS), hydroxyapatite PBS (HA PBS), and silver-containing HA PBS (Ag-HA PBS) groups. The biofilms in the Ti PBS group were clumped and unfocused, whereas those in the HA PBS group were clumped and clear. In the Ag-HA PBS group, the biofilms were scattered and unfocused. The morphological features of the biofilms were observed with a 63× oil objective lens and a zoom factor of 5.0. Scale bar = 2 µm.

bacterial cells whose surface appeared to be unfocused after staining (Figure 2). Meanwhile, those of the Ti PBS group were also composed of clumped bacterial cells with unfocused stained cell surface (Figure 2).

Biofilm analysis using SEM - in vitro experiments. In sharp contrast to the HA PBS group biofilms, those of the Ag-HA PBS group were embedded in less extracellular polymeric substance (EPS), smaller, and appeared to contain scattered bacterial cells (Figure 3). Those of the Ti PBS group were composed of clumped bacterial cells with less EPS (Figure 3). The surface of the Ti disc was flat and smooth.

In contrast, those of the HA disc and the Ag-HA disc were uneven and rough (Figure 3).

Effect of treatments on bacterial survival - in vitro experiments. As confirmed by plating, the discs were inoculated with a mean 43.0 (SD 8.4) $\times 10^7$ CFUs/ml bacterial cells. Mean bacterial counts in the Ti PBS, Ti VCM, HA PBS, HA VCM, Ag-HA PBS, and Ag-HA VCM groups were 2.5 (SD 1.7) $\times 10^7$ CFUs/ml, 27.6 (SD 9.2) $\times 10^6$ CFUs/ml, 42.8 (SD 8.4) $\times 10^6$ CFUs/ml, 3.5 (SD 3.0) $\times 10^7$ CFUs/ml, 3.4 (SD 6.9) $\times 10^4$ CFUs/ml, and 9.5 (SD 8.8) $\times 10^3$ CFUs/ml, respectively (Figure 4a).

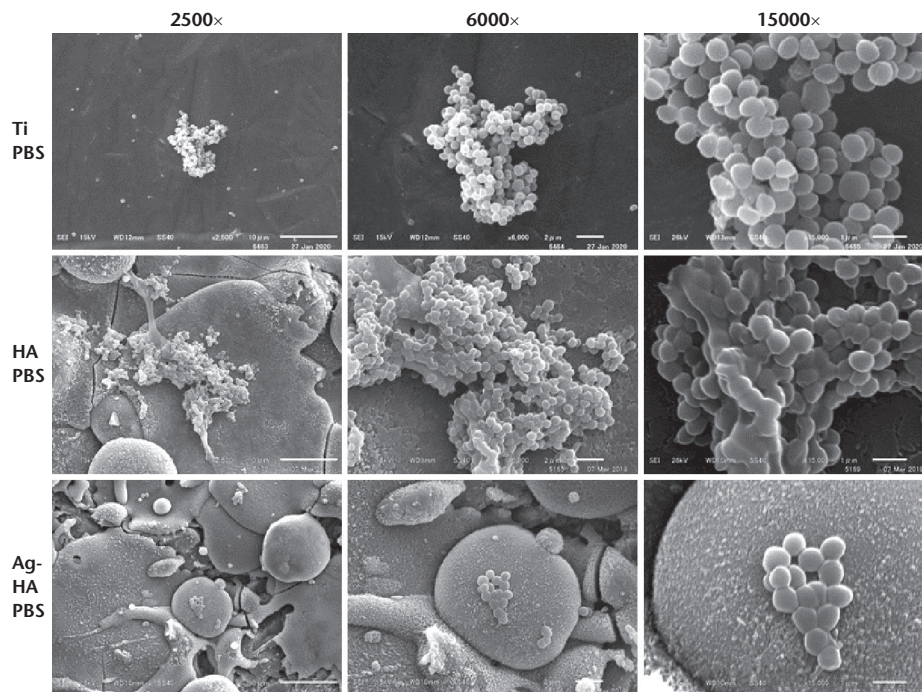


Fig. 3

Scanning electron microscopy (SEM) images of the methicillin-resistant *Staphylococcus aureus* (MRSA) biofilms in the titanium phosphate-buffered saline (Ti PBS), hydroxyapatite PBS (HA PBS), and silver-containing HA PBS (Ag-HA PBS) groups. The magnifications and corresponding scale bars were 2500× and 10 µm, 6000× and 2 µm, and 15000× and 1 µm, respectively. The biofilms in the Ti PBS group were embedded in less extracellular polymeric substance (EPS) and were large, whereas those in the HA PBS group were embedded in large quantities of EPS and were large. In the Ag-HA PBS group, the biofilms were embedded in less EPS and were small and scattered.

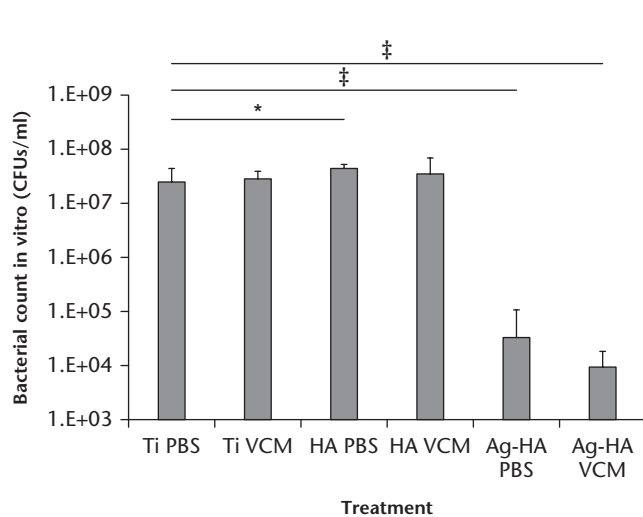


Fig. 4a

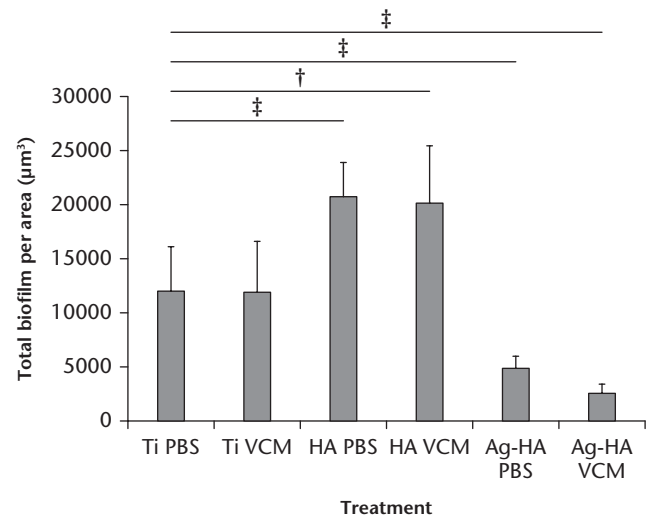


Fig. 4b

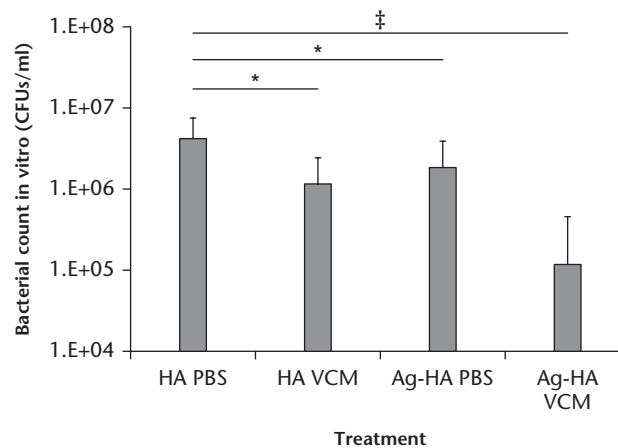


Fig. 4c

The effect of treatments on: a) bacterial survival in vitro; b) biofilm formation; and c) bacterial survival in vivo (total of 12 discs). a) The combination of vancomycin (VCM) and silver (Ag) significantly reduced bacterial cell counts compared to the titanium phosphate-buffered saline (Ti PBS) group ($p < 0.001$, Steel's multiple comparisons test). b) The total biofilm volume in the analyzed area in the Ag-hydroxyapatite PBS (Ag-HA PBS) and Ag-HA VCM groups was significantly smaller than that in the Ti PBS group (12 sections from four discs) ($p < 0.001$, Dunnett's multiple comparison test). c) The effect of VCM with Ag was significantly more reliable than that of either treatment alone (12 discs from three rats) ($p < 0.001$, Steel's multiple comparison test). In all graphs, data are presented as the mean (SD). * $p < 0.05$; ‡ $p < 0.001$.

The bacterial counts of the HA PBS groups were significantly greater than those of the Ti PBS groups ($p = 0.019$, Steel's multiple comparisons test). VCM and Ag have significantly reduced the bacterial cell counts ($p < 0.001$, Steel's multiple comparisons test). There was no significant difference between the bacterial cell counts in the Ti PBS and Ti VCM groups ($p = 0.999$, Steel's multiple comparisons test).

Total biofilm volume using CLSM - in vitro experiments.

The total biofilm volume per area (Figure 4b) was determined based on the analysis of the CLSM images (Figure 5). The mean total biofilm volume per area in the Ti PBS, Ti VCM, HA PBS, HA VCM, Ag-HA PBS, and Ag-HA VCM groups was $12.1 (SD 4.1) \times 10^3 \mu\text{m}^3$, $12.0 (SD 4.7) \times 10^3 \mu\text{m}^3$, $20.9 (SD 3.0) \times 10^3 \mu\text{m}^3$, $20.2 (SD 5.2) \times 10^3 \mu\text{m}^3$, $4.9 (SD 1.1) \times 10^3 \mu\text{m}^3$, and $26.2 (SD 7.6) \times 10^2 \mu\text{m}^3$,

respectively (Figure 4b). The total biofilm volume per area in the Ag-HA PBS and Ag-HA VCM groups was significantly smaller than that in the Ti PBS group ($p < 0.001$, Dunnett's multiple comparisons test). In contrast, those in the HA PBS and HA VCM groups were significantly larger than those in the Ti PBS group ($p < 0.001$ and $p < 0.001$, respectively, Dunnett's multiple comparisons test). There was no significant difference between those in the Ti PBS and Ti VCM groups ($p = 1.000$, Dunnett's multiple comparisons test).

Effect of treatments on bacterial survival - in vivo experiments.

The discs were inoculated with a mean $36.0 (SD 2.1) \times 10^7$ CFUs/ml of bacterial cells. The mean bacterial counts in the HA, HA VCM, Ag-HA, and Ag-HA VCM groups were $4.3 (SD 3.4) \times 10^6$ CFUs/ml, $1.2 (SD 1.3) \times 10^6$ CFUs/ml, $1.9 (SD 2.0) \times 10^6$ CFUs/ml, and $1.2 (SD 3.4) \times 10^5$ CFUs/ml, respectively (Figure 4c). VCM and Ag

significantly reduced bacterial cell counts (VCM: $p = 0.014$; Ag: $p = 0.030$, Steel's multiple comparisons test), and VCM with Ag was more reliable than either of the treatments alone ($p < 0.001$, Steel's multiple comparisons test).

Discussion

In this study, we used 3D CLSM (with and without Airyscan), SEM, and viable cell count analysis to determine the effect of Ag and VCM on MRSA biofilms formed on pure Ti- and HA-coated discs. HA coating for cementless THA has been studied because HA coating induces early bone ingrowth and has good osteoconductivity,⁵ in contrast to Ti implants which showed inferior osteoconductivity.²⁰ Therefore, we used HA-coated discs instead of pure Ti discs as controls *in vivo*.

Methods for qualitative and quantitative biofilm analyses include crystal violet staining, determination of biofilm coverage rates by fluorescence microscopy, and viable cell counting by serial dilution and plating. Each method has its specific strengths and weaknesses.²⁷ CLSM combined with fluorescent staining has recently become a popular method in biofilm studies, and a small number of reports on the determination of biofilm volume have used 3D CLSM assays.^{28,29} To date, only one report on bacterial biofilm analysis by 3D CLSM with Airyscan has been published.³⁰ However, the use of 3D

CLSM with Airyscan and SEM to verify the biofilm analysis findings has not yet been reported.

Biofilm formation can be described as a three-stage process: bacterial adhesion; bacterial aggregation; and biofilm maturation.³¹ Individual, planktonic bacteria start producing EPS after adhesion, which results in bacterium-to-bacterium adhesion. Biofilm thickness is directly proportional to EPS production, and EPS creates a diffusion barrier that prevents the uptake of antibiotics.³² After maturation, the biofilm becomes more resistant to antibiotics.³¹ Conversely, early-stage biofilm is relatively unstable and less resistant to antibiotics than mature biofilm.³¹ As shown in Figure 2, calcein red-orange stained the polysaccharide component of biofilms, i.e. bacteria and EPS. Imaging using 3D CLSM with Airyscan revealed relatively mature biofilms in the Ti PBS group, mature biofilms in the HA PBS group, and early-stage biofilms in the Ag-HA PBS group. SEM observations confirmed that the biofilms formed in the Ag-HA PBS group were thinner and smaller than those formed in the Ti PBS and HA PBS groups. Recently, the antibacterial and antibiofilm activities of Ag were elucidated. Briefly, Ag ions bind to several bacterial cell structures, including peptidoglycans, cell and plasma membranes, DNA, and proteins.^{9,10} Ag delays the growth cycle of biofilms and changes the biofilm structure³³ by facilitating the breakdown of EPS, thereby destabilizing

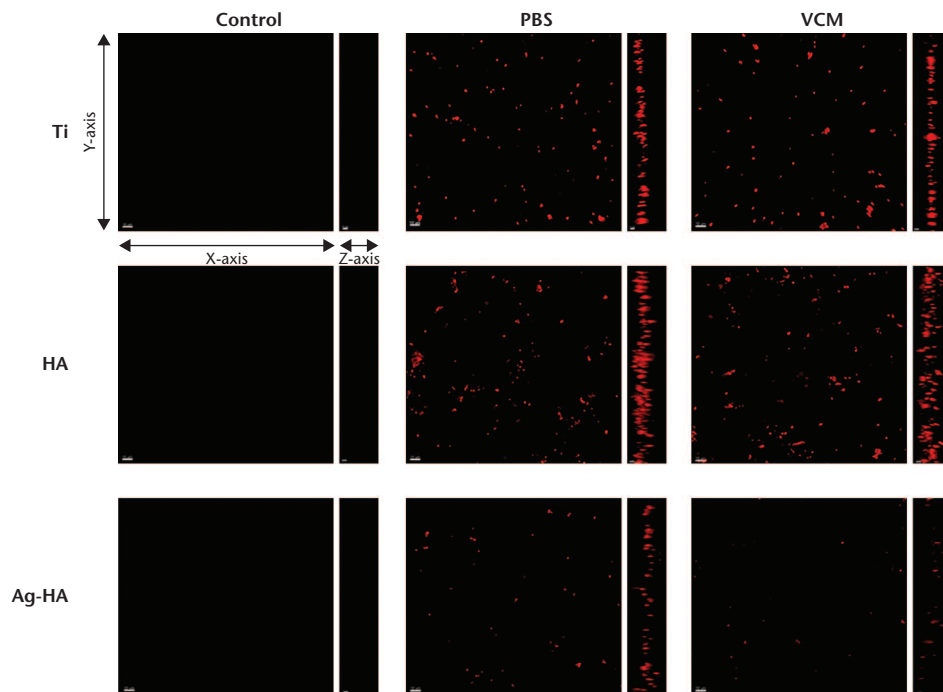


Fig. 5

Confocal laser scanning microscopy (CLSM) images of calcein red-orange-stained methicillin-resistant *Staphylococcus aureus* (MRSA) on discs. The bacteria growth from the following groups are shown: negative control of titanium (Ti), hydroxyapatite (HA) and silver-HA (Ag-HA), Ti phosphate-buffered saline (Ti PBS), Ti vancomycin (Ti VCM), HA PBS, HA VCM, Ag-HA PBS, and Ag-HA VCM. The biofilms were observed with a 20 \times air objective lens and a zoom factor of 2.0. The scale bars on the x and y axes are 10 μ m, whereas that on the z-axis is 5 μ m. The staining intensities of the biofilms are in this order: Ag-HA VCM < Ag-HA PBS < Ti VCM < Ti PBS < HA VCM < HA PBS.

and weakening the biofilm matrix.³⁴ Our findings support the aforementioned Ag antibacterial and antibiofilm activities. Since only one report on bacterial biofilm analysis by 3D CLSM with Airyscan has been published to date,²³ we therefore performed SEM to verify the findings obtained with the 3D CLSM equipped with Airyscan. We obtained similar results with SEM and Airyscan-equipped 3D CLSM; thus, 3D CLSM equipped with Airyscan was a useful method for biofilm observation.

In vitro, VCM has no effect on the viable bacterial counts in the Ti VCM and HA VCM groups compared to those of the Ti PBS group. The viable bacterial counts of the HA PBS group were higher than those of the Ti PBS group. The biofilm formation of the Ti PBS group was smaller than those of the HA PBS and HA VCM groups; nevertheless, VCM had no effect on that of the Ti VCM group. These indicated that biofilms formed on the Ti disc were mature enough to resist VCM, and HA surfaces were more susceptible to bacterial adhesion and biofilm maturation than Ti surfaces. Previous studies have reported biofilm formation on different materials; materials with rough surfaces have greater influence on bacterial adhesion and biofilm maturation than those with smooth surfaces.^{35,36} In the present study, the surfaces of HA and Ag-HA discs were rough whereas those of Ti discs were smooth. Conversely, biofilms formed on Ag-HA discs were immature, and hence both bacterial counts and biofilm formation on Ag-HA discs were significantly suppressed in the presence of VCM compared to those of the Ti PBS group.

In vivo, the viable bacterial counts in the Ag-HA VCM groups were more pronounced than those in the other treatment groups. This indicated that the biofilms on the Ag-HA disc were early stage. The immune defences in vivo combined with antibiotics can contribute to the clearance of bacterial infections.³⁷ Therefore, antibacterial and antibiofilm activities of VCM on HA discs were observed in vivo but not in vitro.

There were several limitations in our study, and additional research will be needed in future to verify our results. First, the combined effect of Ag-HA coating and VCM in the intramedullary implantation model in vivo should be further investigated because of the research of PJI and the difference in VCM distribution between the subcutaneous tissue and bone.^{38–40} Second, the combined effect of Ag-HA coating and VCM should be observed at several periods.³⁸ Third, the other bacterial strains that cause PJI, such as *Staphylococcus epidermidis*, *S. aureus*, *Escherichia coli*, *Enterobacter cloacae*, and *Pseudomonas aeruginosa*, should be tested.^{2,38}

In conclusion, our findings demonstrated the potential synergistic effect between Ag-HA coating and VCM on the reduction of MRSA biofilm formation, which can prove useful for preventing and treating PJI.

Supplementary Material

 Text showing further details regarding the silver-hydroxyapatite (Ag-HA) coating technique, 3D confocal laser scanning microscopy (3D CLSM) and scanning electron microscopy (SEM) protocol, feature of Airyscan, bacterial and culture conditions, and bacterial count determination.

References

- Kurtz S, Ong K, Lau E, Mowat F, Halpern M.** Projections of primary and revision hip and knee arthroplasty in the United States from 2005 to 2030. *J Bone Joint Surg Am.* 2007;89-A(4):780-785.
- González-Vélez AE, Romero-Martín M, Villanueva-Orbaiz R, Díaz-Agero-Pérez C, Robustillo-Rodela A, Monge-Jodra V.** The cost of infection in hip arthroplasty: a matched case-control study. *Rev Esp Cir Ortop Traumatol.* 2016;60(4):227-233.
- Urquhart DM, Hanna FS, Brennan SL, et al.** Incidence and risk factors for deep surgical site infection after primary total hip arthroplasty: a systematic review. *J Arthroplasty.* 2010;25(8):1216-22.e1, 3.
- Berriós-Torres SI, Yi SH, Bratzler DW, et al.** Activity of commonly used antimicrobial prophylaxis regimens against pathogens causing coronary artery bypass graft and arthroplasty surgical site infections in the United States, 2006-2009. *Infect Control Hosp Epidemiol.* 2014;35(3):231-239.
- Suzuki T, Fujibayashi S, Nakagawa Y, Noda I, Nakamura T.** Ability of zirconia double coated with titanium and hydroxyapatite to bond to bone under load-bearing conditions. *Biomaterials.* 2006;27(7):996-1002.
- Lazarinis S, Mäkelä KT, Eskelinen A, et al.** Does hydroxyapatite coating of uncemented cups improve long-term survival? An analysis of 28,605 primary total hip arthroplasty procedures from the Nordic Arthroplasty Register Association (NARA). *Osteoarthritis Cartilage.* 2017;25(12):1980-1987.
- Nishimura S, Tsurumoto T, Yonekura A, Adachi K, Shindo H.** Antimicrobial susceptibility of *Staphylococcus aureus* and *Staphylococcus epidermidis* biofilms isolated from infected total hip arthroplasty cases. *J Orthop Sci.* 2006;11(1):46-50.
- Zhao L, Chu PK, Zhang Y, Wu Z.** Antibacterial coatings on titanium implants. *J Biomed Mater Res B Appl Biomater.* 2009;91(1):470-480.
- Chaloupka K, Malam Y, Seifalian AM.** Nanosilver as a new generation of nanoparticle in biomedical applications. *Trends Biotechnol.* 2010;28(11):580-588.
- Brennan SA, Ní Fhoghlú C, Devitt BM, O'Mahony FJ, Brabazon D, Walsh A.** Silver nanoparticles and their orthopaedic applications. *Bone Joint J.* 2015;97-B(5):582-589.
- Schmidt-Braekling T, Streitberger A, Gosheger G, et al.** Silver-coated megaprotheses: review of the literature. *Eur J Orthop Surg Traumatol.* 2017;27(4):483-489.
- Hussmann B, Johann I, Kauther MD, Landgraaber S, Jäger M, Lendemann S.** Measurement of the silver ion concentration in wound fluids after implantation of silver-coated megaprotheses: correlation with the clinical outcome. *Biomed Res Int.* 2013;2013:763096.
- Fielding GA, Roy M, Bandyopadhyay A, Bose S.** Antibacterial and biological characteristics of silver containing and strontium doped plasma sprayed hydroxyapatite coatings. *Acta Biomater.* 2012;8(8):3144-3152.
- Albers CE, Hofstetter W, Siebenrock KA, Landmann R, Klenke FM.** In vitro cytotoxicity of silver nanoparticles on osteoblasts and osteoclasts at antibacterial concentrations. *Nanotoxicology.* 2013;7(1):30-36.
- Brutel de la Riviere A, Dossche KM, Birnbaum DE, Hacker R.** First clinical experience with a mechanical valve with silver coating. *J Heart Valve Dis.* 2000;9(1):123-129.
- Tweden KS, Cameron JD, Razzouk AJ, Holmberg WR, Kelly SJ.** Biocompatibility of silver-modified polyester for antimicrobial protection of prosthetic valves. *J Heart Valve Dis.* 1997;6(5):553-561.
- Wan AT, Conyers RA, Coombs CJ, Masterton JP.** Determination of silver in blood, urine, and tissues of volunteers and burn patients. *Clin Chem.* 1991;37(10 Pt 1):1683-1687.
- Noda I, Miyaji F, Ando Y, et al.** Development of novel thermal sprayed antibacterial coating and evaluation of release properties of silver ions. *J Biomed Mater Res B Appl Biomater.* 2009;89(2):456-465.

19. Shimazaki T, Miyamoto H, Ando Y, et al. In vivo antibacterial and silver-releasing properties of novel thermal sprayed silver-containing hydroxyapatite coating. *J Biomed Mater Res B Appl Biomater*. 2010;92(2):386-389.
20. Yonekura Y, Miyamoto H, Shimazaki T, et al. Osteoconductivity of thermal-sprayed silver-containing hydroxyapatite coating in the rat tibia. *J Bone Joint Surg Br*. 2011;93-B(5):644-649.
21. Tsukamoto M, Miyamoto H, Ando Y, et al. Acute and subacute toxicity in vivo of thermal-sprayed silver containing hydroxyapatite coating in rat tibia. *Biomed Res Int*. 2014;2014:902343.
22. Ando Y, Miyamoto H, Noda I, Sakurai N. Calcium phosphate coating containing silver shows high antibacterial activity and low cytotoxicity and inhibits bacterial adhesion. *Mater Sci Eng C*. 2010;30(1):175-180.
23. Klinger-Strobel M, Stein C, Forstner C, Makarewicz O, Pletz MW. Effects of colistin on biofilm matrices of *Escherichia coli* and *Staphylococcus aureus*. *Int J Antimicrob Agents*. 2017;49(4):472-479.
24. Hahnel S, Ionescu AC, Cazzaniga G, Ottobelli M, Brambilla E. Biofilm formation and release of fluoride from dental restorative materials in relation to their surface properties. *J Dent*. 2017;60:14-24.
25. Kawai S, Takagi Y, Kaneko S, Kurosawa T. Effect of three types of mixed anesthetic agents alternate to ketamine in mice. *Exp Anim*. 2011;60(5):481-487.
26. Thompson JM, Saini V, Ashbaugh AG, et al. Oral-only linezolid-rifampin is highly effective compared with other antibiotics for periprosthetic joint infection: study of a mouse model. *J Bone Joint Surg Am*. 2017;99-A(8):656-665.
27. Klinger-Strobel M, Suesse H, Fischer D, Pletz MW, Makarewicz O. A novel computerized cell count algorithm for biofilm analysis. *PLoS One*. 2016;11(5):e0154937.
28. Kommerein N, Doll K, Stumpp NS, Stiesch M. Development and characterization of an oral multispecies biofilm implant flow chamber model. *PLoS One*. 2018;13(5):e0196967.
29. Fish KE, Collins R, Green NH, et al. Characterisation of the physical composition and microbial community structure of biofilms within a model full-scale drinking water distribution system. *PLoS One*. 2015;10(2):e0115824.
30. Thomsen H, Graf FE, Farewell A, Ericson MB. Exploring photoinactivation of microbial biofilms using laser scanning microscopy and confined 2-photon excitation. *J Biophotonics*. 2018;11(10):e201800018.
31. Gbejuade HO, Lovering AM, Webb JC. The role of microbial biofilms in prosthetic joint infections. *Acta Orthop*. 2015;86(2):147-158.
32. Costerton JW, Stewart PS, Greenberg EP. Bacterial biofilms: a common cause of persistent infections. *Science*. 1999;284(5418):1318-1322.
33. Guo J, Qin S, Wei Y, et al. Silver nanoparticles exert concentration-dependent influences on biofilm development and architecture. *Cell Prolif*. 2019;52(4):e12616.
34. Chaw KC, Manimaran M, Tay FE. Role of silver ions in destabilization of intermolecular adhesion forces measured by atomic force microscopy in *Staphylococcus epidermidis* biofilms. *Antimicrob Agents Chemother*. 2005;49(12):4853-4859.
35. Schmidlin PR, Müller P, Attin T, Wieland M, Hofer D, Guggenheim B. Polyspecies biofilm formation on implant surfaces with different surface characteristics. *J Appl Oral Sci*. 2013;21(1):48-55.
36. Al-Ahmad A, Wiedmann-Al-Ahmad M, Fackler A, et al. In vivo study of the initial bacterial adhesion on different implant materials. *Arch Oral Biol*. 2013;58(9):1139-1147.
37. Shen F, Tang X, Cheng W, et al. Fosfomycin enhances phagocyte-mediated killing of *Staphylococcus aureus* by extracellular traps and reactive oxygen species. *Sci Rep*. 2016;6:19262.
38. Moriarty TF, Harris LG, Mooney RA, et al. Recommendations for design and conduct of preclinical in vivo studies of orthopedic device-related infection. *J Orthop Res*. 2019;37(2):271-287.
39. Kobatake T, Miyamoto H, Hashimoto A, et al. Antibacterial activity of Ag-hydroxyapatite coating against hematogenous infection by methicillin-resistant *Staphylococcus aureus* in the rat femur. *J Orthop Res*. 2019;37(12):2655-2660.
40. Bue M, Tøttrup M, Hanberg P, et al. Bone and subcutaneous adipose tissue pharmacokinetics of vancomycin in total knee replacement patients. *Acta Orthop*. 2018;89(1):95-100.

Author information

- A. Hashimoto, MD, Graduate Student,
- T. Kobatake, MD, Graduate Student,
- T. Nakashima, MD, Graduate Student,
- M. Ueno, MD, PhD, Orthopedic Surgeon,
- M. Sonohata, MD, PhD, Associate Professor,
- M. Mawatari, MD, PhD, Professor, Department of Orthopaedic Surgery, Faculty of Medicine, Saga University, Saga, Japan.
- T. Shobuiki, PhD, Assistant Professor,
- H. Miyamoto, MD, PhD, Professor, Department of Pathology and Microbiology, Faculty of Medicine, Saga University, Saga, Japan.
- T. Murakami, PhD, Visiting Researcher, Department of Pathology and Microbiology, Faculty of Medicine, Saga University, Saga, Japan; Research Section, Medical Division, KYOCERA Corporation, Yasu, Japan.
- I. Noda, MS, Visiting Researcher, Department of Pathology and Microbiology, Faculty of Medicine, Saga University, Saga, Japan; Research Section, Medical Division, KYOCERA Corporation, Yasu, Japan.

Author Contributions

- A. Hashimoto: Designed the research, Acquired and interpreted the data, Drafted the manuscript.
- H. Miyamoto: Designed the research, Interpreted the data, Revised the manuscript critically.
- T. Kobatake: Acquired the data.
- T. Nakashima: Acquired the data.
- T. Shobuiki: Acquired the data.
- M. Ueno: Designed the research, Acquired the data.
- T. Murakami: Acquired the data.
- I. Noda: Designed the research.
- M. Sonohata: Drafted the manuscript.
- M. Mawatari: Designed the research, Interpreted the data.

Funding statement

- No benefits in any form have been received or will be received from a commercial party related directly or indirectly to the subject of this article.

Conflict of interest statement

- None declared

Acknowledgements

- None declared

Ethical review statement

- All animal procedures were conducted with the approval of the Animal Research Ethics Committee of our institution (approval number 29-044-0).

©2020 Author(s) et al. This is an open-access article distributed under the terms of the Creative Commons Attribution Non-Commercial No Derivatives (CC BY-NC-ND 4.0) licence, which permits the copying and redistribution of the work only, and provided the original author and source are credited. See <https://creativecommons.org/licenses/by-nc-nd/4.0/>.